Experimental and numerical investigation on the behavior of reinforced reactive powder concrete two-way slabs under static load

Hala A. Hamid
B.Sc., Civil Engineering Department
College of Engineering-University of Baghdad
civilengineer_hala@yahoo.com

Dr.Shatha D. Mohammed
Asst. Prof., Civil Engineering Department
College of Engineering-University of Baghdad
shathadhia@yahoo.com

Abstract: -

This paper studied the behaviour of reinforced reactive powder concrete (RPC) two-way slabs under static load. The experimental program included testing three simply supported slabs of 1000 mm length, 1000 mm width, and 70 mm thickness. Tested specimens were of identical properties except their steel fibers volume ratio (0.5 %, 1 %, and 1.5 %). Static test results revealed that, increasing steel fibers volume ratio from 0.5% to 1% and from 1% to 1.5%, led to an increase in: first crack load by (32.2 % and 52.3 %), ultimate load by (36.1 % and 17.0 %), ultimate deflection by (33.6 % and 3.4 %), absorbed energy by (128 % and 20.2 %), and the ultimate strain by (1.1 % and 6.73 %). The stiffness and ductility of the specimens also increased. A numerical analysis was performed using ANSYS 14.5 software. The FE analysis overestimated the ultimate load capacity of all specimens by (6–28) %, and underestimated the ultimate deflection by (22-44) %. The deflected shape and crack patterns of the FE models were similar to that of the corresponding experimental specimens. It was found out that the optimum values of steel fibers volume fraction are 1.5 % and 1.6%.

Keywords: Mechanical properties of RPC, reactive powder concrete, steel fibres, steel fibres modelling, two-way slab.

Introduction

The tensile strength of the ordinary concrete has some unfavourable outcomes on its performance as an important building and construction material. This involves the necessity for steel reinforcement and sometimes huge section members which are aesthetically unfavourable and consume large amounts of materials. Reactive Powder Concrete (RPC) is an emerging technology has the ability to overcome the aforementioned handicaps, where it can be used to

create small section members with high efficiency.

RPC is usually formed from extremely fine powder materials (cement, sand, quartz powder and silica fume), steel fibers (optional) and superplasticizer [14]. By optimizing the granular packing of the dry fine powders, a material of very small amounts of defects such as micro-cracks and voids in a comparison with the conventional concrete can be achieved. RPC has a very good durability because of its low and non-connected porosity and due to its perfect impermeability, Hence; it has been used for isolation and containment of nuclear waves [12].

Steel fibres are usually added. The fibrous RPC that produced under a good quality control condition, has a very good mechanical properties, where it has a high tensile strength, and its compressive and flexural strengths reach 800 MPa and 40 MPa respectively [11], also it has ductility and energy absorption values approaching those of steel material [10]. Khadhum, 2014 [8] studied experimentally, the behaviour of RPC two-way slabs of different curing conditions. It was concluded that increasing micro-steel fibers content causes an increase in stiffness, ultimate load, deflection, and ductility of the slab specimens, and delays the cracks propagation and control their growth. Also, it was found out that using heat treatment method increases the first crack and the ultimate load of specimens.

Tu'ma , 2016 [9] and Kamonna, 2010 [4] modeled numerically the steel fibers by two methods using ANSYS software, the first method was inserting the steel fibers as a smeared reinforcement in SOLID65 element (the element that was used to represent the concrete material), and examining six different ways of steel fibers distribution, plain concrete element (without steel fibers), horizontal one-layer, vertical one-layer, inclined one layer, equally two-way distribution (two layers ,vertical and horizontal) , and three-way distribution (three layers, vertical, horizontal and inclined). The second method was inserting the enhanced final mechanical properties of concrete due to the steel fibers existence. The analysis results revealed that the first method is better than the second, and its results were closer to the experimental results. The analysis results revealed also that, in general, the distribution of steel fibers in two equal layers in two directions is more convenient.

This paper studies, experimentally, the behaviour of Reactive Powder Concrete two-way slabs under static load, and presents a finite element simulation for the specimens.

The Experimental Program

i. Materials

Ordinary Portland cement (Type-I), natural sand of maximum particle size smaller than 1.18 mm, silica fume (SF), tap water, and SikaViscocrete-5930 superplasticizer (SP) were used to produce the RPC mix for all the specimens. Discontinuous discrete hooked end steel fibers of 1mm diameter, 30 mm length, and ultimate tensile strength of (1100) MPa were added. The mix proportions of the used RPC mix are shown in **Table. 1**

Table. 1 Mix proportions of the used RPC mix.

Material	Proportion
cement	750 kg/m^3
sand	1200 kg/m^3
SF	200 kg/m^3
w/b*	0.2
SP	2% binder weight

* Water to binder ratio

ii. Test specimens

Three simply supported RPC two-way slabs have been cast and tested. All of their geometrical, material properties, and reinforcement details were identical except the steel fibers volume fraction (0.5 %, 1 %, and 1.5 %). The specimens were identified by two terms, the first term is "S" which refers to the static load, and the second is the steel fibers volume fraction. Dimensions and some other details of the slab specimens are illustrated in **Fig. 1**. All the specimens were reinforced by one layer of 6 mm diameter deformed rebars (f_y =420 MPa) at 170 mm c/c spacing in both directions.

iii. Instrumentation

A number of measurement tools and instruments were used to conduct the experimental work of this research such as strain, deflection, load, and crack width measurements. One electrical strain gauge (5 mm) was installed in each reinforcement mesh at the mid of the closest bar to the plate of loading, three strain gauges (20 mm) were installed at the bottom face of each slab specimen.

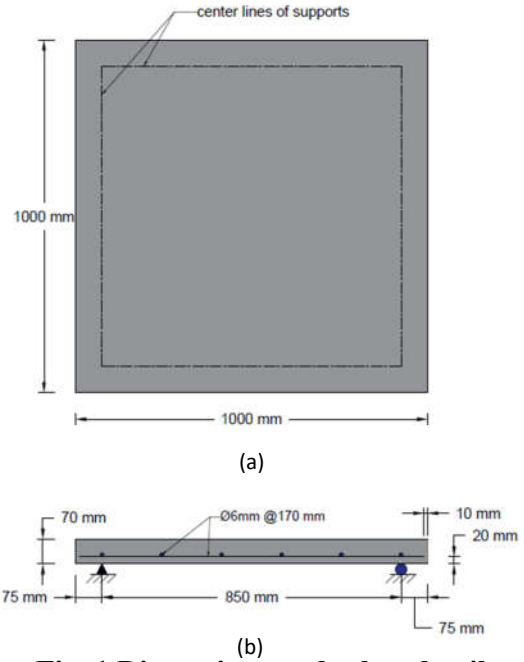

Fig. 1 Dimensions and other details of the slab specimens: (a) Top view, (b) Sectional view.

Two dial gauges of 0.01 mm sensitivity, were installed for measuring the vertical deflection in two locations, the first one was in the center of the slab bottom face, to measure the downward deflection, and the other was installed above the support to measure the uplift. A tool consists of twenty metal slices of different thicknesses ranging from 0.05 mm to 1 mm was used to measure the width of cracks. The locations of the concrete strain gauges and the dial gauges are shown in **Fig. 2**, where the strain gauges are marked with rectangular shape.

iv. Testing Procedure

All specimens were prepared for the test by painting the surfaces by white color and installing the strain gauges in their right locations at the bottom face of the slab specimen. After that, the specimen was placed in its right position on the testing frame so that the support lines of the frame were identical with those of the slab specimen. Thereafter; loading plate and dial gauges were fixed in their specified positions **Fig. 3.**

In the static load test the specimen was loaded gradually till failure stage. The load was applied with an increment of approximately (300 kg/ 10 min) using a hydraulic jack and a load cell of 200 Ton capacity. After each loading step, the magnitude of the applied load, vertical deflection at the center of the slab, uplift of the supports, cracks width, crack patterns, and strain in both steel reinforcement and concrete surface were recorded.

Test Results and Discussion

i. Static Test Results

Static test program included examining three reinforced RPC two-way slab specimens. A flexural failure occurred in all the tested slab specimens, the cracks were initially formed in the bottom face of the slab under the loading plate (where the maximum bending occurred and tensile stress exceeded the concrete modulus of rupture) then radiated to the edges of the slab. It was observed that for all the tested specimens, when the first crack initiated, it was of a very small width (smaller than 0.05 mm) and its shape was close to a polygon with short crack lines initiated from its corners and extended towards the slab edges.

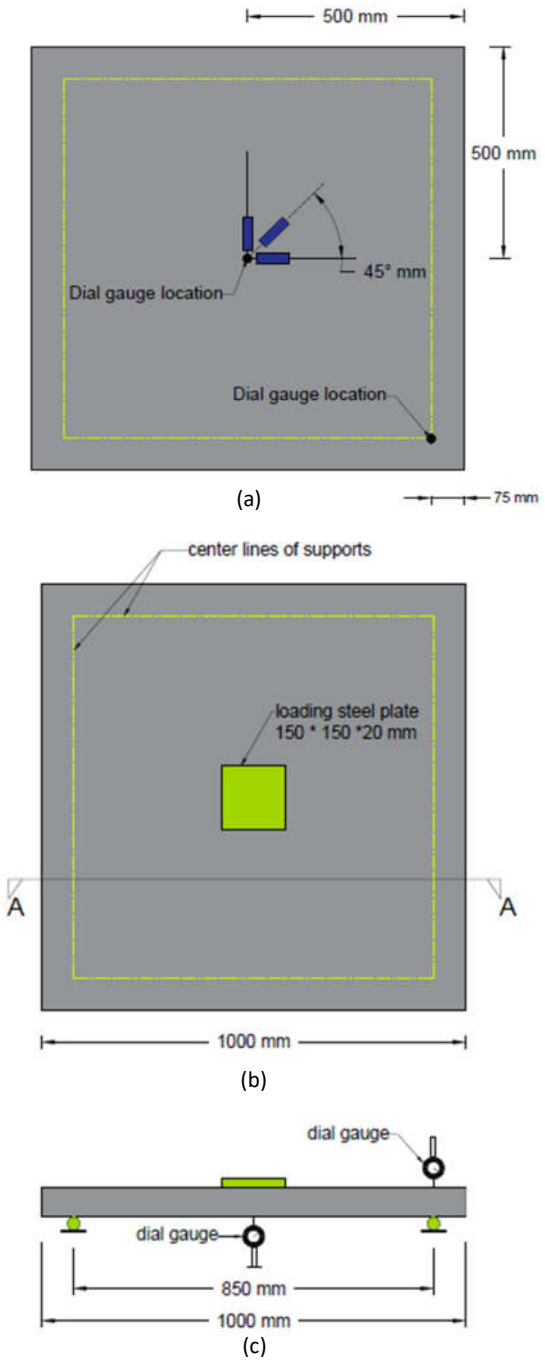

Fig. 2 Schemes of the test set-up: (a) view of bottom face, (b) view of top face, (c) Section A-A.

Fig. 3 Specimen test set-up.

This crack layout is compatible with the state of loading and boundary conditions of the slabs.

With increasing load, the cracks along the diagonals of the tension face widened and extended, then a number of new additional cracks were formed in the central region of the tension face. At higher load, the central deflection increased and the cracks along the diagonals propagated and extended till they reached to the slab corners and passed through the slab sides toward the upper face of the slab. At the final stages of the loading, the steel reinforcement yielded, excessive deflections was observed, the generated cracks widened and spread progressively till the bottom face of the slab was filled with cracks in all directions and the slab was no longer carry any loads and failure occurred. **Fig. 7** shows the crack pattern of the

tension face for the tested specimens after failure.

Test results revealed that, increasing steel fibers volume fraction from 0.5% to 1% and from 1% to 1.5%, led to an increase in the first crack load (load that recorded when first crack generated at the bottom face of specimen) and the ultimate load by (32.2 % and 52.3 %) and (36.1 % and 17.0 %) respectively, as it is illustrated in **Table. 2**. It was noticed that the widths of the cracks of all the tested specimens remained small till the final stages of loading, where they were approximately equal to (0.2 mm) at a loading stage of (80-85 %) from the ultimate load. This caused by the presence of the steel fibers which delayed the propagation of the cracks and controlled their growth.

Table. 2 Cracking and ultimate load for the experimental specimens.

Specimen	P_{cr} (kN)	% Increase in P_{cr}	P_u (kN)	% Increase in P_u	% P_{cr}/P_u
S0.5%	14.9	-	54.0	-	29.8
S1%	19.7	32.2 %	73.5	36.1 %	26.8
S1.5%	30.0	52.3 %	86.0	17.0 %	34.9

Test results also revealed that, increasing steel fibers volume fraction from 0.5% to 1% and from 1% to 1.5%, led to an increase in the deflections at first crack by 4.8% and 36.4 % respectively, and also led to an increase in the ultimate deflection as illustrated in **Table. 3**. It was noticed that the increase of the ultimate deflection, when steel fibers volume fraction increased from 0.5 % to 1 %, was clear and significant (33.6 %), however; it was small when steel fibers volume fraction increased from 1% to 1.5% (3.4%). For S1% and S1.5% specimens, when they gradually loaded, the deflection was still increased linearly as the load increased even after the first cracks generation by high stages of loading, while for S0.5%, the load-deflection relation was linear only before the first cracks generation as it clear in **Fig. 4**, and that belongs to the effect of the steel fibers which increased the stiffness of the concrete. It was also clear from **Fig. 4** that, the slope of the linear parts is directly proportion with the steel fibers volume fraction which also belonged to the influence of steel fibers that is increased the stiffness of the concrete. After the longitudinal reinforcement had yielded and the steel fibers pullout reached its final stage, the deflection increased continuously without an appreciable increment in the load. The rate of deflection increasing was so fast at the ultimate load of all the specimens and no reliable data could be recorded at this stage, for this reason, all load-deflection curves had been terminated at the last load step before failure.

Table. 3 Central deflection of the experimental specimens.

Spec.	Deflection at first crack (mm)	% Increase	Ultimate deflection (mm)	% Increase
S0.5 %	2.1	-	11.0	-
S1%	2.2	4.8 %	14.7	33.6 %
S1.5 %	3.0	36.4 %	15.2	3.4 %

Test results indicated that increasing steel fibers volume fraction from 0.5% to 1.5%, decreased the principal strain at the first crack due to the effect of the steel fibers on increasing the stiffness of the specimens .This result is compatible with the linear behaviour of the load-deflection curve for S1% and S1.5% specimens. However; the ultimate principal strains had increased as the steel fibers volume fraction increased due to the positive effect of the steel fibers on the ductility of the specimens as shown in **Table. 4** and **Fig. 5**.

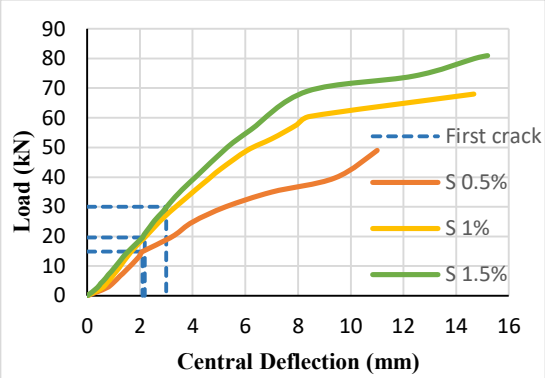

Fig. 4 Load-Defection curves of the experimental specimens.

Table. 4 Principal strain at first crack and ultimate load for the experimental specimens.

Specimen	Principal strain at first crack	Ultimate principal strain	% Increase in ultimate principal strain
S0.5%	0.005	0.01690	-
S1%	0.00023	0.01708	1.1 %
S1.5%	0.00015	0.01823	6.73 %

The load-strain behaviour of the steel reinforcement for S1% and S1.5% specimens is shown in **Fig. 6**, no strain data could be obtained for S0.5%, because the steel reinforcement strain gauge for this specimen was damaged. It was achieved from the experimental data that the yielding strain of the steel reinforcement is approximately equal to 0.00226, it is marked with red dashed lines in **Fig. 6.**

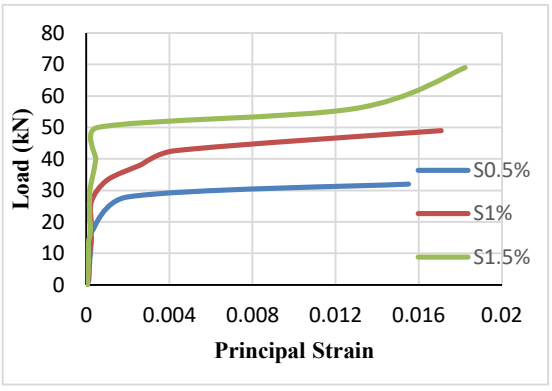

Fig. 5 Load-strain curves of the bottom face for all RPC slab specimens of the experimental specimens.

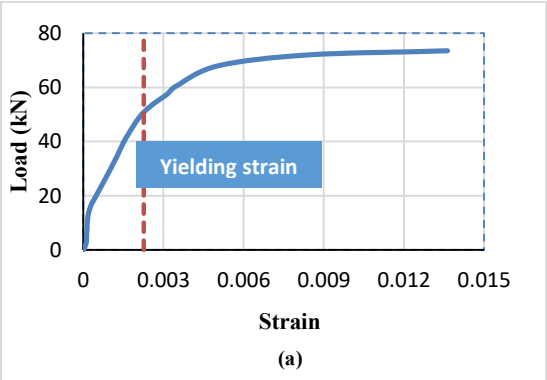

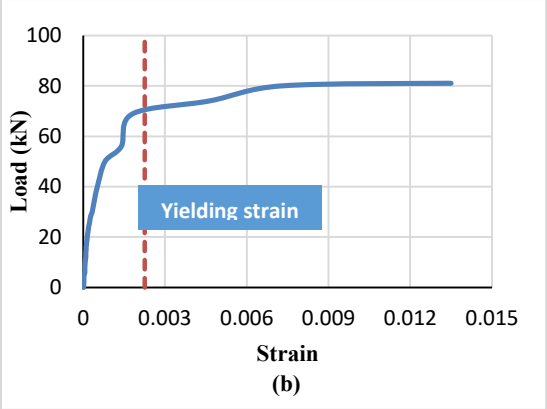

Fig. 6 Load-Strain curves of the steel reinforcement of: (a) S1%, (b) S1.5% specimens.

Flexural toughness is the total energy that can be absorbed by the specimen before failure, which can be calculated from the area under the load-deflection curve in flexure [3]. Test results showed that the absorbed energy is directly proportion with the percentage of the steel fibres volume fraction, where when the steel fibers volume fraction was increased from 0.5% to 1% and from 1% to 1.5%, the absorbed energy increased by 128 % and 20.2% respectively, as it is shown in **Table. 5**.

Table. 5 Absorbed energy of the experimental specimens.

Specimen	Absorbed energy (kN . mm)	% Increase
S0.5%	300.8	-
S1%	685.9	128.0 %
S1.5%	824.5	20.2 %

The Numerical Analysis

i. Modeling

Mechanical APDL ANSYS 14.5 software was used to simulate the behaviour of the experimental specimens.

SOLID65, LINK180, and SOLID185 elements were used to represent the RPC, steel reinforcement, and loading steel plate respectively. **Discrete model** [13] was used to represent the behaviour of steel reinforcement.

All the required real constants of the materials were inserted. The effect of steel fibers on the structural behaviour of the slabs had been simulated by modeling the steel fibers as a smeared layer in SOLID65 element, as a ratio from the element volume, where the SOLID65 supports up to three different rebar specifications in three directions [2].

(a)

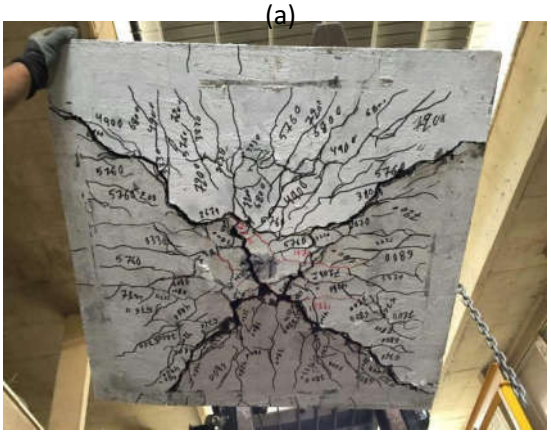

(b)

(c)

Fig. 7 Crack pattern of the tension face for the experimental specimens: (a) S0.5%, (b) S1%, and (c) S1.5%.

These specifications can be controlled by controlling the three options of SOLID65 real constants: rebar1, rebar2, and rebar3. Through these options, the material, volume ratio, orientation angles of steel fibers can be controlled, where the material number refers to the model number of steel fiber material which must be already defined. The volume ratio represents the ratio of steel fibers to the SOLID65 element volume. The horizontal and the vertical orientation angles represent the alignment direction of steel fibers inside the SOLID65 element. All the vertical angles were set to zero, because it is observed during the experimental work, in the casting process, that the steel fibers tend to align to the horizontal plane. The horizontal angles were set to (0^o, 45^o, and 90^o). In other words, the horizontal and vertical angles were inserted as (0 & 0), (45 & 0) and (90 & 0) for rebar1, rebar 2, and rebar 3 respectively.

Material nonlinearity for some of the used materials had been considered, hence; multiple definitions were needed for each one of them. The material of steel reinforcement bars had defined as bilinear isotropic material. It was required to define (EX) for the linear part, which was represented the modulus of elasticity of the steel (E_s) and was taken as 200000 MPa. PRXY is the Poisson's ratio of the steel, and it was taken as 0.3 [7]. It was also required to define the yield stress (f_y) and tangent modulus, 420 MPa and zero were inserted for them.

Steel fibers material was also modeled as a bilinear isotropic material. (200000 MPa, 0.3, 420 MPa, and 0) were inserted to be their modulus of elasticity, Poisson's ratio, yield stress, and tangent modulus respectively. The material of the loading plate was defined as linear isotropic material. The adopted modulus of elasticity and Poisson's ratio of this material were (200000 MPa, and 0.3) respectively.

Multiple definitions were required to define the RPC material such as the definition of the linear and multi-linear isotropic properties. To define the multi-linear isotropic properties, two models were adopted to simulate the uniaxial compressive stress-strain behaviour of RPC:

- **Al-Hassani, 2015 model**

A regression analysis to get a curve fitting model for expressing the complete compressive stress-strain relationship of RPC mixes was carried out by (Al-Hassani et al, 2015) [5]. The following nonlinear equation was obtained:

$$f_c = f'_c \times \left[\frac{a \left(\frac{\varepsilon_c}{\varepsilon_o}\right)^b}{c + \left(\frac{\varepsilon_c}{\varepsilon_o}\right)^d} \right] \qquad (1)$$

Where, f_c is the compressive stress of concrete (MPa), ε_c is the compressive strain of concrete. f'_c ,ε_o are the experimental compressive strength (MPa) and its corresponding strain respectively.

$a = 3.805$, $b = 0.919$, $c = 2.831$, $d = 3.970$

Equation (1) has been used in the present study to obtain the compressive stress-strain curve as shown in **Table. 6**

Additional constants were needed to be defined for modeling the RPC in the present study:

1- Shear transfer coefficient for an open crack (β_o), C1.

2- Shear transfer coefficient for a closed crack (β_c), C2.

3- Uniaxial tensile cracking stress (f_{ct}), C3.

4- Uniaxial crushing stress (f'_c), C4.

β_o and β_c coefficients are usually varied between 0-1, and β_c is greater than β_o. The zero value means that the crack is smooth while the unity value (1.0) means that the crack is rough. In the present finite element analysis, the same of the experimental values of f_{ct} and f'_c are adopted.

MacGregor, J.G., 1992 model

A nonlinear equation to obtain the compressive uniaxial stress-strain curve of concrete was proposed by (MacGregor, J.G., 1992) [6]:

$$f = \frac{E_c\,\varepsilon}{1+\left(\frac{\varepsilon}{\varepsilon_o}\right)^2} \qquad (2)$$

Where;

$$\varepsilon_o = \frac{2\,f'_c}{E_c} \qquad (3)$$

f is the stress at any strain, ε is the strain at any stress, and ε_o is the strain at ultimate compressive strength f'_c.

Table. 6 Material properties of concrete based on *Al-Hassani* model.

Mat. model No.	Element type	Material properties		
65	SOLID65	Linear Isotropic		
		EX	25796	
		PRXY	0.2	
		Multilinear Isotropic		
		Points	Strain	Stress
		Point 1	0	0
		Point 2	0.0005	13.21
		Point 3	0.0006	16.37
		Point 4	0.0010	23.60
		Point 5	0.0014	32.47
		Point 6	0.0016	38.11
		Point 7	0.0023	51.06
		Point 8	0.0026	55.27
		Point 9	0.0029	59.18
		Point 10	0.0035	63.76
		Point 11	0.0036	64.58
		Point 12	0.0037	64.70
		Point 13	0.0038	64.70
		Concrete		
		β_o	0.000001	
		β_c	0.00001	
		f_{ct}	4.35	
		f'_c	64.7	

The static modulus of elasticity of concrete was determined from the following equation [1]:

$$\begin{aligned} E_c &= 4700\sqrt{f'_c} \quad f'_c < 41.6\ MPa \\ &= [3.32\sqrt{f'_c} + 6.895]\left(\frac{w_c}{2320}\right)^{1.5} \quad f'_c \geq 41.6\ \text{MPa} \end{aligned} \qquad (4)$$

The second equation was adopted since the compressive strength of all the specimens were greater than 41.6 MPa. All of the required properties are listed in **Table. 7**.

The RPC slab, loading plate, and support shafts were modeled as volumes **Fig. 8**. All the volumes were meshed with a square element of 20 mm edge length as shown in **Fig. 9**, the lines of reinforcement bars had also meshed with 20 mm element length. The proper mesh attributes were given to each element. The bottom edges of the supporting shaft were constrained to simulate the simple support condition, where two of the shafts were constrained in x-, y-, and z-directions to be the hinges, while the remaining two shafts were constrained in (x, y) and (z, y) directions respectively to be the rollers. Load was applied as a pressure on the top area of the loading steel plate.

ii. Analysis Results

The numerical analysis was overestimated the ultimate load capacity of the slab specimens as it is clear from **Table. 10**. It was noticed that the first crack load resulted from the numerical analysis was almost the same for all the models (approximately 30 kN), and this value was close to the experimental first crack load for S1.5 % specimen only, while it was much higher than the experimental first crack load of the remaining specimens as is clear from **Table. 9**.

Table. 7 Material properties of concrete based on *MacGregor J.G.*, model.

Mat. model No.	Element type	Material properties		
65	SOLID65	Linear Isotropic		
		EX	36844	
		PRXY	0.2	
		Multilinear Isotropic		
		Points	Strain	Stress
		Point 1	0	0
		Point 2	0.0005	18.86
		Point 3	0.0006	23.54
		Point 4	0.0010	33.67
		Point 5	0.0014	44.57
		Point 6	0.0016	50.38
		Point 7	0.0023	60.28
		Point 8	0.0026	62.47
		Point 9	0.0029	64.02
		Point 10	0.0035	65.00
		Concrete		
		β_o	0.00001	
		β_c	0.0001	
		f_{ct}	4.35	
		f'_c	65	

As it is clear from **Table. 10**, the numerical analysis was underestimated the ultimate deflection of all the models except S1.5% model, where the numerical (based on Al-Hassani model) and the experimental ultimate deflection of this model were the same. As it is clear from **Fig. 10**, the load-deflection curves that obtained from the numerical analysis were extremely different than the corresponding experimental curves, they were much stiffer especially at the elastic stage as it is shown in **Fig. 8** and **Fig. 11**.

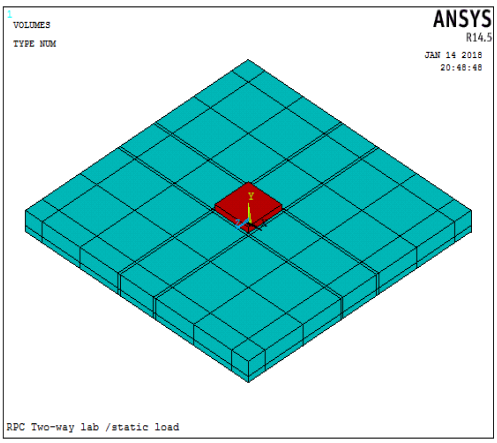

Fig. 8 Created volumes of the RPC slab and steel plate of loading.

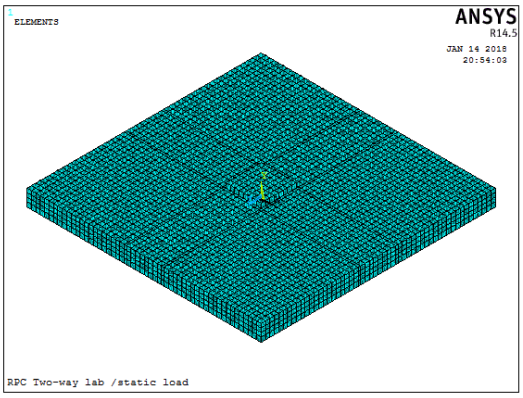

Fig. 9 Meshed volumes.

The deflected shape pattern that resulted from the numerical analysis was similar to that of the experimental one, where the maximum deflection was occurred at the center of the slabs under the loading plate, while there was an uplift occurred at the corners and edges of the slabs. For example **Fig. 12** shows the deflected shape of the model S1.5 %.

Table.8 Comparison between the numerical and the experimental ultimate load capacity.

Specimen	Experimental ultimate load, (kN)	Numerical ultimate load, (kN)	P_{num}/P_{exp}
***Al-Hassani* model**			
S0.5%	**54.0**	68.9	1.28
S1%	**73.5**	82.3	1.12
S1.5%	**86.0**	93.0	1.08
***MacGregor* model**			
S0.5%	**54.0**	67.0	1.24
S1%	**73.5**	78.1	1.06
S1.5%	**86.0**	98.1	1.14

Table.9 Comparison between the numerical and the experimental first crack load.

Specimen	Experimental first crack load, (kN)	Numerical first crack load, (kN)	P_{num}/P_{exp}
***Al-Hassani* model**			
S0.5%	14.9	30.6	2.05
S1%	19.7	30.7	1.56
S1.5%	30.0	30.5	1.01
***MacGregor* model**			
S0.5%	14.9	30.5	2.05
S1%	19.7	30.7	1.56
S1.5%	30.0	30.5	1.01

The crack pattern of the numerical ANSYS models was also similar to that of the experimental specimens.

From the above-mentioned results and observations, it is concluded that the finite element analysis was overestimated the maximum load capacity, and underestimated the ultimate deflection of all models. Also, the finite element models were extremely stiffer than the experimental specimens. There are a number of reasons for these results:

Table.10 Comparison between the numerical and the experimental ultimate deflection.

Specimen	Experimental ultimate deflection, (mm)	Numerical ultimate deflection, (mm)	def_{num}/def_{exp}
***Al-Hassani* model**			
S0.5%	11.0	7.6	0.69
S1%	14.7	9.6	0.65
S1.5%	15.2	15.2	1.0

MacGregor model			
S0.5%	11.0	8.4	0.76
S1%	14.7	8.2	0.56
S1.5%	15.2	11.9	0.78

1- The steel fibers are perfectly distributed inside the concrete, that makes the concrete an isotropic material and that is not realistic.

2- The method of support simulation, where, in the finite element modeling, the supports were prevented the movement of the slab in both upward and downward directions, while the real supports were prevented the vertical movement in the downward direction only.

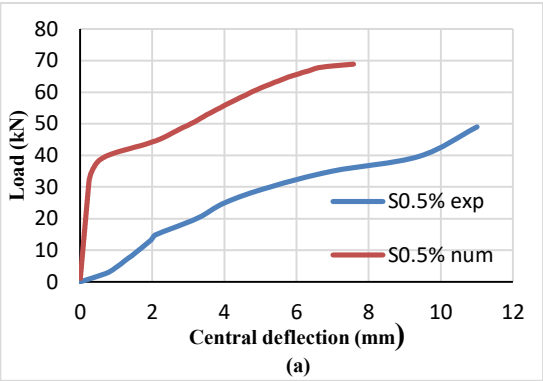

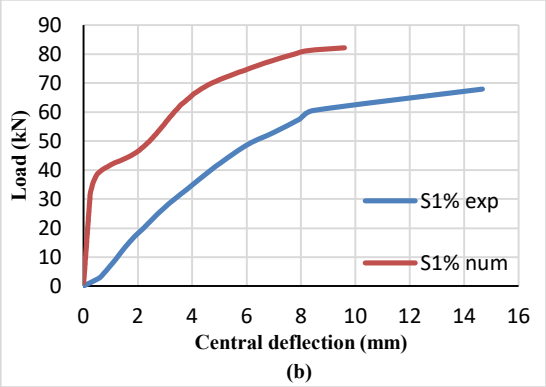

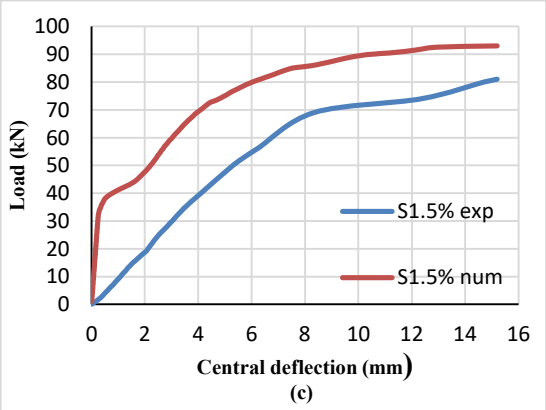

Fig. 10 Comparison between the numerical and experimental load-deflection curves for the static test specimens based on *Al-Hassani* model.

3- The finite element analysis does not take the cracks that caused by shrinkage and handling into a consideration, however; the Reactive Powder Concrete usually experience a high shrinkage because it contains a high rate of fine materials.

4- In the finite element analysis, the steel reinforcement was assumed to be perfectly bonded with the concrete,

while in the actual situation, a slipping occurs to some extent.

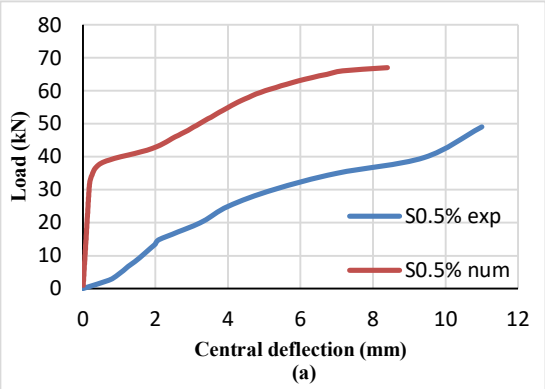

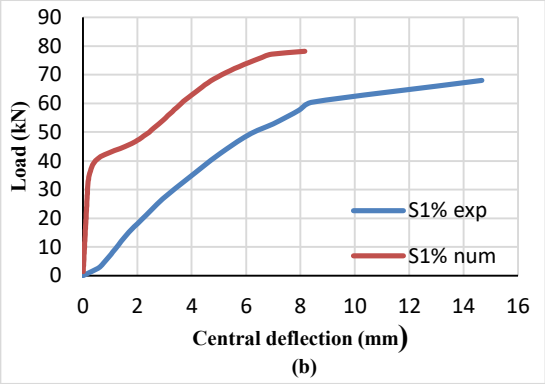

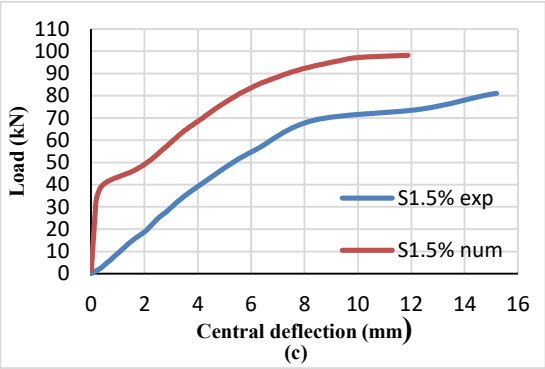

Fig. 11 Comparison between the numerical and experimental load-deflection curves for the static test specimens based on *MacGregor* model.

iii. Parametic Study: The effect of changing the steel fiber volume fraction

Different values of steel fibers volume fractions **Table. 13** were examined to investigate the effect of changing the steel fibers volume fraction on the behaviour of reinforced RPC two-way slab under static load.

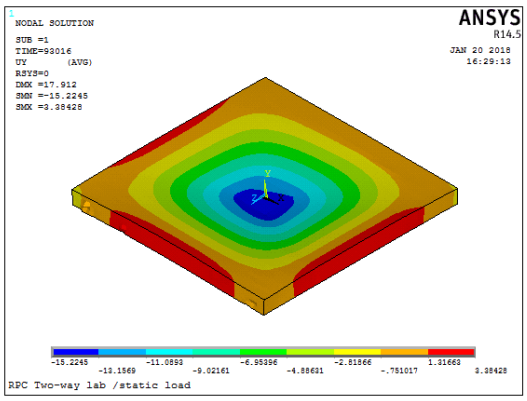

Fig. 12 Deflected shape of S1.5 % model at ultimate load based on Al-Hassani model.

This parametric study was depended on ***Al-Hassani*** model. From **Table. 11**, it can be concluded that the optimum values of steel fiber volume fraction are 1.5 % and 1.6%, because these two models had resisted the maximum deflections among the models before failure (15.2 mm, and 14.9 mm respectively), also they had a relatively high ultimate load capacities at the same time (93 kN, and 97 kN respectively) in a comparison with other specimens.

It is concluded that increasing the steel fibers volume fraction to a specific

level significantly improves the mechanical properties of concrete and the structural behaviour of the concrete elements, however; further increasing of the volume fraction leads to negative effects such as decreasing the ductility of concrete and difficulties of casting and handling of the fresh concrete because a congestion occurs by the fibers. It was observed that all the numerical models were approximately of the same initial stiffness, as it clear from **Fig. 13**, increasing the steel fibers volume fraction had no effect on the load-deflection behaviour at the elastic stage, while the effect was clear and significant at the final stages of loading. This can be the reason of why the first crack load was the same for all the models (30 kN), while the first crack load of the experimental specimens was different (14.9 kN, 19.7 kN, and 30.0 kN for S0.5%, S1%, and S1.5% respectively), that can be due to the modeling method of the steel fibers as it mentioned previously.

Table. 11 Ultimate load and ultimate deflection for the numerical models of different steel fibers volume fraction.

Specimen	Ultimate load, (kN)	Ultimate deflection, (mm)
S0%	46.0	4.5
S0.5%	68.9	7.6
S1%	82.3	9.6
S1.5%	93.0	15.2
S1.6%	97.6	14.9
S1.7%	89.5	8.9
S1.8%	96.8	10.0
S1.9%	99.0	11.62
S2%	99.8	10.4

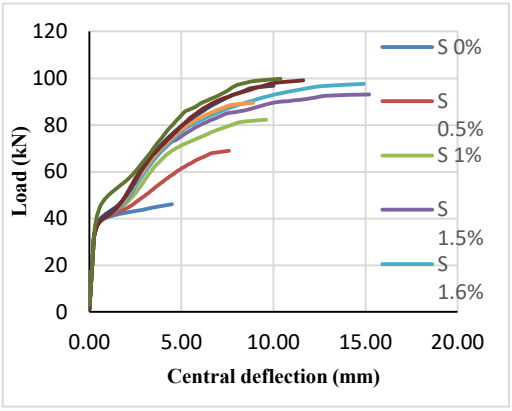

Fig. 13 he effect of changing the steel fibers volume fraction on the load-deflection curves of the numerical models.

Conclusions

1- Static test results revealed that increasing steel fibers volume fraction from 0.5% to 1% and from 1% to 1.5%, led to an increase in the: first crack load by (32.2 % & 52.3 %), ultimate load by (36.1 % & 17.0 %), ultimate deflection by (33.6 % & 3.4 %), absorbed energy by (128 % & 20.2 %), and the ultimate strain by (1.1 % & 6.73 %). It also increased the stiffness and the ductility of the specimens especially at the final stages of loading. Additionally, it delayed the propagation of the cracks, controlled their growth, kept the integrity of the specimens at post cracking stage, and avoided their ruin at the failure

stage through its "bridging" effect.

2- The finite element analysis overestimated the ultimate load capacity of all specimens, where the ultimate load that based on *Al-Hassani* and *MacGregor* models was greater than the experimental ultimate load by (8-28) % and (6-24) % respectively.

3- The first crack load that resulted from the numerical analysis was almost the same for all models (approximately 30 kN), and this value was close to the experimental first crack load for S1.5 % specimen only, while it was much higher than the experimental first crack load of the remaining specimens.

4- The crack pattern of all the finite element models was similar. However; the model S1.5% resisted much cracking in a comparison with the other models, and this is compatible with the experimental results, where when the steel fibers volume fraction was increased, the ductility increased and the specimens resist more cracking before failure.

5- The deflected shape pattern that resulted from the numerical analysis was similar to that of the experimental one, where the maximum deflection was occurred at the center of the slabs under the loading plate, while there was an uplift occurred at the corners and edges of the slabs.

6- The numerical analysis underestimated the ultimate deflection of all the models except S1.5% model, where the numerical (based on *Al-Hassani* model) and the experimental ultimate deflection of this model were the same. However; for S0.5%, and S1% models, the numerical ultimate deflection based on *Al-Hassani* model was smaller than the corresponding experimental by 31% and 35% respectively. While the numerical analysis that depended on *MacGregor* model was underestimated the ultimate deflection of all specimens by (22-44) %.

7- The finite element models were extremely stiffer than the experimental specimens for many reasons, such that:

- The method of steel fibers modeling, as it previously mentioned, the steel fibers were modeled as a smeared layer in SOLID65 element in three distribution ways of equal ratios in each way. In other words, the steel fibers are perfectly distributed inside the concrete, that makes the concrete

an isotropic material and that is not realistic.

- The method of support simulation, in the finite element modeling, the supports were prevented the movement of the slab in both upward and downward directions, while the real supports were prevented the vertical movement in the downward direction only.

- The finite element analysis does not take the cracks that caused by shrinkage and handling into a consideration, however; the Reactive Powder Concrete usually experience a high shrinkage because it contains a high rate of fine materials.

- In the finite element analysis, the steel reinforcement was assumed to be perfectly bonded with the concrete, while in the actual situation, a slipping occurs to some extent.

- There is an approximation in the modeling of the used materials, especially the modeling of the multi-linear isotropic properties of RPC and the modeling of steel fibers behaviour.

8- Based on the parametric study that examined the effect of changing the steel fibers volume fraction on the behaviour of the specimens, it was found out that the optimum values of steel fibers volume fraction are 1.5 % and 1.6%.

9- Increasing the steel fibers volume fraction to a specific level (which is 1.5 % and 1.6% in the present study) significantly improves the mechanical properties of concrete and the structural behaviour of the concrete elements, however; further increasing of the volume fraction leads to negative effects such as decreasing the ductility of concrete and difficulties of casting and handling of the fresh concrete due to the congestion that is caused by the fibers.

References: -

[1] ACI 435 (1995) Control of deflection in concrete Structure.

[2] ANSYS Mechanical APDL 14.5 Help (2012).

[3] Design considerations for steel fiber reinforced concrete (1999).ACI 544.4R-88 Report.

[4] Kamonna H. H. (2010) Non-linear analysis of fibrous reinforced concrete deep beams using ANSYS software. Kufa Journal of Engineering. 2(1), 109-124.

[5] Al-Hassani H. M., Khalil W. I, & Danha L. S. (2015) Proposed model for

uniaxial compression behaviour of Reactive Powder Concrete. Journal of Babylon University,Engineering Sciences. 23(3).

[6] MacGregor, J.G. (1992) Reinforced concrete mechanics and design. Prentice-Hall, Inc., Englewood Cliffs. NJ, 848.

[7] Merritt F. S., & Ricketts J.T. (2001) Building Design and Construction Handbook, Sixth Edition. McGraw-Hill.

[8] Khadhum M. (2014) Performance of Reactive Powder Concrete slabs with different curing conditions. Journal of Engineering and Technology Research. 6(6), 81-93.

[9] Tu'ma N. H. (2016) Behaviour of Reactive Powder Concrete beams reinforced with fiber reinforced polymer bars. Ph.D. Thesis/ Civil Engineering department /Collage of Engineering/ University of Baghdad.

[10] Lee N.P., & Chisholm D.H. (2005) Reactive Powder Concrete. BRANZ Study Report 146.

[11] Blais P. Y., & Couture M. (1999) Precast prestressed pedestrian bridge world's first Reactive Powder Concrete structure. PCI Journal. 44(5), 60-71.

[12] Mohammed S. D., Majeed W. Z., Naji N. B., & Fawzi N. M. (2017) Investigating the influence of gamma ray energies and steel fibre on attenuation properties of reactive powder concrete . Nuclear Science and Techniques. 28 (10): 153.

[13] Tavarez, F. A. (2001) Simulation of behaviour of composite grid reinforced concrete beams using explicit Finite flement method. M. Sc. Thesis, University of Wisconsin-Madison.

[14] Bonneau O., Vernet C., Moranville M., & Aitcin P. (2000) Characterization of the granular packing and percolation threshold of reactive powder concrete. Cement and Concrete Research. 30(12), 1861-1867.

دراسة عملية وعددية لسلوك سقوف خرسانة المساحيق الفعّالة المسلّحة ثنائية الاتجاه تحت تأثير الأحمال الساكنة

هالة عقيل حامد
بكالوريوس، قسم الهندسة المدنية
كلية الهندسة / جامعة بغداد

د. شذى ضياء محمد
أستاذ مساعد، قسم الهندسة المدنية
كلية الهندسة / جامعة بغداد

الخلاصة: -

يدرس هذا البحث سلوك سقوف خرسانة المساحيق الفعّالة المسلّحة ثنائية الاتجاه تحت تأثير الأحمال الساكنة. تضمّن البرنامج العملي فحْصَ ثلاثة سقوف مسلّحة ثنائية الاتجاه بسيطة الإسناد، بطول 1000 ملم ، عرض 1000 ملم ، و سمك 70 ملم. كانت جميع النماذج ذات خصائص متطابقة ما عدا محتوى الألياف الفولائية (0.5 %، 1 %، 1.5 %). أظهرت نتائج الفحص الستاتيكي أنّ زيادة النسبة الحجمية للألياف الفولاذية من 0.5 % إلى 1% ، و من 1% إلى 1.5% أدّت إلى زيادة: حمل التشقق الأدنى بمقدار (32.2% و 52.3) و الحمل الأقصى للفشل بمقدار (36.1% و 17.0%) و الهطول الأقصى بمقدار (33.6% و 3.4%) و الطاقة الممتصة بمقدار (128% و 20.2%) و الإنفعال الأقصى بمقدار (1.1% و 6.73%). كما أنها زادت من متانة الخرسانة و مطيليتها.

تمّ استخدام التحليل العددي (طريقة العناصر المحددة) باستخدام برنامج ANSYS 14.5 لمحاكاة تصرف النماذج العملية. كان حمل الفشل الأقصى الناتج من التحليل العددي أعلى من الناتج عملياً بمقدار (6-28) %،اما الهطول الأقصى للنماذج فكان أقل من الناتج عملياً بمقدار (22-44)%. بالنسبة لشكل التشوه و انماط توزيع الشقوق و الصدوع الناتجة من التحليل العددي فقد كانت مشابهة للناتجة عملياً. أظهر التحليل العددي أن النسب الحجمية المثلى للألياف الفولاذية هي 1.5% و 1.6%.

الكلمات المفتاحية: - الخصائص الميكانيكية لخرسانة المساحيق الفعالة، خرسانة المساحيق الفعالة، الألياف الفولاذية، نمذجة الالياف الفولاذية، السقوف ثنائية الاتجاه.